

# Design and Implementation of a Takum Arithmetic Hardware Codec in VHDL

Laslo Hunhold 

**Abstract**—The takum machine number format has been recently proposed as an enhancement over the posit number format, which is considered a promising alternative to the IEEE 754 floating-point standard. Takums retain the useful posit properties, but feature a novel exponent coding scheme that yields more precision for small and large magnitude numbers. Takum’s dynamic range is larger and bounded, as reflected in its name, derived from the Icelandic ‘*takmarkað umfang*’, meaning ‘limited range’. Consequently, the selection of bit string lengths becomes determined solely by precision requirements and independent of dynamic range considerations. Takum is defined in both a logarithmic number system (LNS) format and a traditional floating-point format.

This paper presents the design and implementation of a hardware codec for both the logarithmic and floating-point takum formats. The design primarily focuses on the codec, as both formats share a common internal arithmetic representation. Non-essential aspects of current posit designs, such as fused or pipelined architectures and the choice of floating-point IP cores, are thus omitted. The proposed takum codec, implemented in VHDL, demonstrates near-optimal scalability and performance on an FPGA, matching or exceeding state-of-the-art posit codecs in terms of both latency and LUT utilisation.

**Index Terms**—machine numbers, takum arithmetic, posit arithmetic, logarithmic number system, floating-point arithmetic, HDL, VHDL, FPGA

## I. INTRODUCTION

For decades, IEEE 754 floating-point numbers have been the dominant format for representing real numbers in computing. However, recent demands for low- and mixed-precision arithmetic in fields such as machine learning have highlighted significant shortcomings of the IEEE 754 standard, particularly in terms of reproducibility, precision and dynamic range. While modifications within the IEEE 754 framework, such as Google’s `bf16` [1], have been proposed to address these issues, more fundamental changes to computer arithmetic are also being explored.

One such innovation is posit arithmetic [2], [3], which has garnered significant attention in recent years. Posits have *tapered precision* by encoding the exponent with variable length, allowing for more fraction bits around numbers near 1, at the expense of fewer fraction bits for numbers of very small or large magnitude. This encoding also allows treating posits like two’s complement integers in terms of sign, ordering and negation.

The author is with the Department of Mathematics and Computer Science, University of Cologne, 50969 Cologne, Germany (e-mail: hunhold@uni-koeln.de)

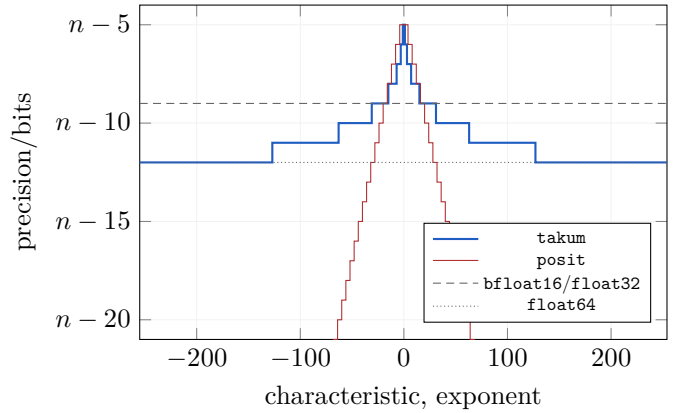


Figure 1: Precision (number of mantissa/fraction bits) depending on the respective coded characteristic or exponent for takum, posit and a selection of floating-point formats.

The posit format is generally considered simpler to implement in hardware compared to IEEE 754 floating-point numbers, largely due to the reduction of special cases. Over the past few years, several optimised hardware implementations have been developed. Initial work is documented in [4], [5], with further optimisations leading to the creation of the FloPoCo posit core generator [6]–[9]. This culminated in the development of a complete RISC-V posit core supporting up to 64-bit precision [10], [11].

Despite the potential of posits in various low- and mixed-precision applications [12], [13], several challenges have hindered their adoption. Chief among these is the sharp decline in precision for small and large magnitude numbers (Figure 1), which poses significant problems for general-purpose arithmetic. This limitation is compounded by a lack of dynamic range at lower bit counts (Figure 2), where the fraction bit count can drop to zero, resulting in an unbounded relative approximation error. Consequently, many established numerical methods cannot be directly applied to posits [14], [15].

In response to these challenges, the takum format was recently proposed [15] as a solution. Takum introduces a new encoding scheme that guarantees a minimum of  $n - 12$  fraction bits (Figure 1) and achieves a significantly increased dynamic range that is fully realised at 12-bit precision, remaining constant thereafter (Figure 2). This design not only makes takum suitable for applying well-established numerical analysis techniques, but it also decouples the choice of precision from dynamic range concerns in mixed-precision applications. This property is re-

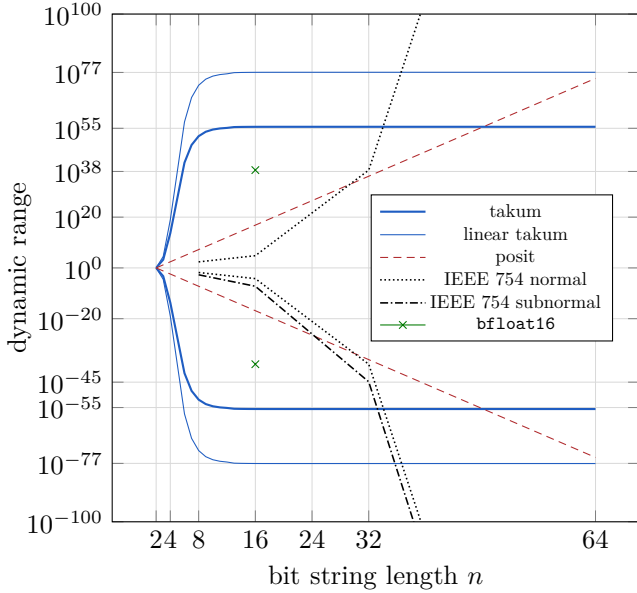


Figure 2: Dynamic range relative to the bit string length  $n$  for takum, posit and a selection of floating-point formats.

flected in its name, derived from the Icelandic ‘*takmarkað umfang*’, meaning ‘limited range’.

An additional design aspect of takum is that it is defined as a logarithmic number system (LNS) by default, while also being usable as a traditional floating-point format (‘linear takum’). LNSs have been shown to be advantageous in terms of energy efficiency and hardware complexity (see [16]–[19] and [15, Section 4.3] for further discussion).

While the takum format has been formally verified [15], its hardware implementation has only been briefly touched upon in [15, Section 5.2], with claims that it should be simpler than posit implementations. The primary reason is that the takum exponent is limited to 11 bits, as opposed to potentially occupying the entire width of a posit. As a result, the bit string length in takum should have minimal impact on the complexity of encoding and decoding processes, unlike in posit arithmetic. However, the upfront computational costs of takum encoding and decoding remain an open question.

This paper makes three primary contributions: (1) we mathematically derive efficient algorithms for encoding and decoding takum numbers; (2) we provide a detailed pseudocode description and an open-source VHDL implementation optimised for FPGA hardware; and (3) we compare the performance of the takum codec with state-of-the-art posit codecs, demonstrating advantages in both latency and LUT utilisation.

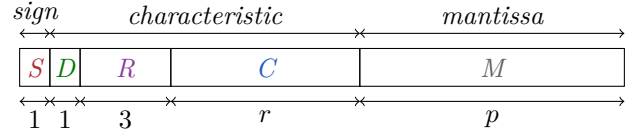
The remainder of this paper is organised as follows: Section II defines the takum format in both its default logarithmic and linear forms. Section III introduces a novel internal representation for logarithmic number systems, inspired by recent advances in posit codecs. Sections IV and V then detail the design and implementation of a takum decoder and encoder, respectively. Section VI

presents an evaluation of the VHDL implementation on FPGA, followed by a conclusion and outlook in Section VII.

## II. TAKUM ENCODING SCHEME

We begin by defining the takum encoding scheme. As previously mentioned, takum is primarily defined as a LNS, though we will also provide takum’s linear definition later, which closely resembles the logarithmic form.

**Definition 1** (takum encoding [15, Definition 2]). *Let  $n \in \mathbb{N}$  with  $n \geq 12$ . Any  $n$ -bit MSB→LSB string  $T := (S, D, R, C, M) \in \{0, 1\}^n$  of the form*



with sign bit  $S$ , direction bit  $D$ , regime bits  $R := (R_2, R_1, R_0)$ , characteristic bits  $C := (C_{r-1}, \dots, C_0)$ , mantissa bits  $M := (M_{p-1}, \dots, M_0)$ , regime

$$r := \begin{cases} \text{uint}(\bar{R}) & D = 0 \\ \text{uint}(R) & D = 1 \end{cases} \in \{0, \dots, 7\}, \quad (1)$$

characteristic

$$c := \begin{cases} -2^{r+1} + 1 + \text{uint}(C) & D = 0 \\ 2^r - 1 + \text{uint}(C) & D = 1 \end{cases} \in \{-255, \dots, 254\}, \quad (2)$$

mantissa bit count  $p := n - r - 5 \in \{n - 12, \dots, n - 5\}$ , mantissa  $m := 2^{-p} \text{uint}(M) \in [0, 1)$  and logarithmic value

$$\ell := (-1)^S (c + m) \in (-255, 255) \quad (3)$$

encodes the takum value

$$\tau(T) := \begin{cases} \begin{cases} 0 & S = 0 \\ \text{NaN} & S = 1 \end{cases} & D = R = C = M = 0 \\ (-1)^S \sqrt{e}^\ell & \text{otherwise} \end{cases} \quad (4)$$

with  $\tau: \{0, 1\}^n \mapsto \{0, \text{NaN}\} \cup \pm (\sqrt{e}^{-255}, \sqrt{e}^{255})$  and EULER’s number  $e$ . Without loss of generality, any bit string shorter than 12 bits is also considered in the definition by assuming the missing bits to be zero bits (‘ghost bits’).

As can be observed, takums are defined for any  $n \in \mathbb{N}_1$ , in contrast to IEEE 754 floating-point numbers, which are restricted to specific values of  $n \in \{16, 32, 64, \dots\}$ . The linear definition of takums closely mirrors the logarithmic one:

**Definition 2** (linear takum encoding [15, Definition 20]). *Take Definition 1 and rename the mantissa bit count  $p$ , mantissa bits  $M$  and mantissa  $m$  to fraction bit count  $p$ , fraction bits  $F$  and fraction  $f$ . Define the exponent*

$$e := (-1)^S (c + S) \in \{-255, \dots, 254\} \quad (5)$$

and the linear takum value encoding as

$$\hat{\tau}(T) := \begin{cases} \begin{cases} 0 & S = 0 \\ \text{NaR} & S = 1 \end{cases} & D = R = C = F = \mathbf{0} \\ [(1 - 3S) + f] \cdot 2^e & \text{otherwise.} \end{cases} \quad (6)$$

As we can see, both the logarithmic and linear definitions of takum are largely similar. In this paper, we will adhere closely to both definitions for the development of the codec. To provide an overview of their numerical properties, refer to Figure 1, which compares the precision, i.e., the number of available mantissa/fraction bits, across various machine number formats as a function of the coded exponent. Takums exhibit a tapering of precision similar to that of posits. However, a notable distinction is that takum precision is bounded from below, unlike posits, which rapidly lose precision for larger coded exponents. Notably, takums always provide at least as many mantissa/fraction bits as `float64`, meaning that linear takums have at least equivalent machine precision. Consequently, classical results in numerical analysis for `float64` are directly applicable to `takum64`.

Figure 2 presents another comparison, focusing on dynamic range. Takums demonstrate a bounded dynamic range that is quickly reached and nearly fully available even at  $n = 8$ . In contrast, posits exhibit limited dynamic range for  $n < 32$ , only slightly surpassing that of IEEE 754 floating-point numbers, which also have insufficient dynamic range for  $n < 32$ . The dynamic range of `float64` is excessively large and is not shown here. For a detailed discussion on the rationale behind the dynamic range of takum, refer to [15].

The bounded and rapidly achieved dynamic range of takums provides a significant advantage: the choice of machine number format becomes a matter of precision alone, rather than a trade-off between precision and dynamic range. This feature could be particularly beneficial in mixed-precision arithmetic applications.

### III. INTERNAL REPRESENTATION

While it is clear that the decoder’s input, as well as the encoder’s output, is a binary representation of a takum, defining the decoder’s output and encoder’s input in general cases is more complex. This internal representation must not only uniquely identify a takum but also facilitate efficient arithmetic operations. Typically, decoders and encoders are used as input and output stages within an arithmetic unit, so the internal representation should be optimised for these contexts.

In the linear case, the most straightforward approach would be to use the standard floating-point internal representation of the form

$$(S, \tilde{e}, \tilde{f}) \mapsto (-1)^S (1 + \tilde{f}) \cdot 2^{\tilde{e}} \quad (7)$$

with  $\tilde{f} \in [0, 1)$  and  $\tilde{e} \in \{-254, \dots, 254\}$ . However, as demonstrated by Yonemoto [2] for the default internal

representation of posits and further generalised by [9], it is more effective to adopt the internal representation

$$(S, e, f) \mapsto [(1 - 3S) + f] \cdot 2^e \quad (8)$$

with  $f \in [0, 1)$  and  $e \in \{-255, \dots, 254\}$ . This choice is advantageous because the internal representation is monotonic in  $f$ , similar to how the fraction bits  $F$  are monotonic in takum encoding. This monotonicity avoids the need for a full two’s complement negation of the fraction during decoding and encoding when  $S$  is 1, as would be necessary with the representation in (7). The trade-off between (7) and (8) involves a slightly more complex arithmetic for the latter and a departure from the extensive body of work associated with the former, as discussed in [8], [9]. Moreover, examining the exponent definition,  $e = (-1)^S(c + S)$ , reveals that it simplifies to  $c$  when  $S = 0$  and  $-c$  when  $S = 1$ , corresponding to a simple binary negation in hardware.

Turning to the logarithmic case, the canonical internal representation is given by

$$(S, \ell) \mapsto (-1)^S \sqrt{e}^\ell \quad (9)$$

where  $\ell \in (-255, 255)$ , consistent with the definition. This representation is also utilised in the most recent work on logarithmic posits [13]. However, this approach has a drawback similar to the linear case, as it necessitates a full two’s complement negation both after decoding to and before encoding from the internal representation. By definition,  $\ell = (-1)^S(c + m)$ . An alternative we propose here is to define a ‘barred logarithmic value’ as  $\bar{\ell} := c + m = (-1)^S \ell \in (-255, 255)$  and use the internal representation

$$(S, \bar{\ell}) \mapsto (-1)^S \sqrt{e}^{(-1)^S \bar{\ell}}. \quad (10)$$

The advantage of this novel representation is that  $\bar{\ell}$  is monotonic in  $m$ , just as the mantissa bits  $M$  are monotonic in takum encoding. This monotonicity eliminates the need for two’s complement negations after decoding and before encoding. The impact on arithmetic complexity is minimal, as all sign cases of  $\ell$  must be handled regardless. For instance, when computing the square root, which involves a right shift of  $\ell$ , the procedure remains unchanged. Similarly, multiplication and division require handling all sign combinations of  $\ell$ , as does addition and subtraction.

The barred logarithmic value  $\bar{\ell}$  can be easily derived from  $c$  and  $m$  by concatenating the 9-bit signed integer  $c$  with the  $n - 5$ -bit unsigned integer  $2^{n-5} \cdot m$  (given  $p + r = n - 5$ ), which is then interpreted as an  $n + 4$ -bit fixed-point number. In general, whether in the linear or logarithmic case, the internal representations  $(S, e, f)$  and  $(S, \bar{\ell})$  are straightforward to determine from the characteristic  $c$  and the equivalent fraction  $f$  and mantissa  $m$ .

### IV. DECODER

The purpose of the decoder is to transform a given  $n$ -bit takum binary representation, where  $n \in \mathbb{N}_2$ , into its corresponding internal representation. Specifically, this

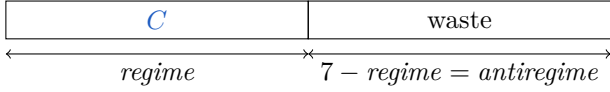


Figure 3: Bit layout of  $characteristic\_raw\_bits \in \{0, 1\}^7$ . The 0 to 7 characteristic bits  $C$  are followed by 7 to 0 bits of waste.

internal representation is expressed as  $(S, e, f)$  in the linear case and as  $(S, \bar{\ell})$  in the logarithmic case (see (8) and (10)). As demonstrated in Section III, both forms of internal representation can be directly derived from the characteristic  $c$  and the mantissa  $m$  (where the fraction  $f$  corresponds to  $m$ ). Consequently, our primary objective is to determine  $c$  and  $m$ , as they serve as the common foundation for both cases. Once these values are established, the respective internal representations can be subsequently derived. Additionally, if the input corresponds to a special representation, such as 0 or NaR, this should also be appropriately flagged.

Given that takums are a tapered precision machine number format, it is also essential to determine the number of mantissa bits (precision) for a given input. The direction bit  $D$  (*direction\_bit*) and the sign bit  $S$  (*sign*) can be straightforwardly extracted from the two most significant bits (MSBs) of the input. Therefore, for the purposes of this discussion, we shall assume that these bits are readily available.

#### A. Characteristic/Exponent Determinator

To determine the characteristic (and later, the exponent), we focus on the following problem reduction: Referring to the takum bit pattern defined in Definition 1 and considering that both the characteristic length and the bit pattern are variable, it is most effective to expand the bit pattern to 12 bits and then extract the 7 bits that follow the regime. This extraction will be carried out later; our current focus is on the processing of these bits.

These 7 bits, which we refer to as the raw characteristic (*characteristic\_raw\_bits*), are guaranteed to include all the characteristic bits, followed by a variable number of unused bits (referred to as waste). This is illustrated in Figure 3. By construction, the number of characteristic bits corresponds to the value of *regime*, while the number of waste bits is given by  $7 - regime$ . We define the latter as the *antiregime*.

If we examine the definition of the characteristic provided in (2), we observe that it involves introducing a bias to the characteristic bits. This process entails a bitwise operation, followed by either an increment or a decrement of the bits. To simplify the procedure and avoid the need for decrements, we propose a normalisation approach that exclusively relies on increments. To justify this approach, we first present the following

**Proposition 1** (characteristic negation). *Let  $n \in \mathbb{N}_1$  and  $T := (S, D, R, C, M) \in \{0, 1\}^n$  as in Definition 1 with*

Table I: All possible biases  $-2^{r+1}$  given as 9-bit two's complement integers for all regimes  $r$  ranging from 0 to 7. The  $r$  least significant bits are underlined.

$r$	$-2^{r+1}$
0	111111110
1	11111110 <u>0</u>
2	1111110 <u>00</u>
3	111110 <u>000</u>
4	11110 <u>0000</u>
5	1110 <u>00000</u>
6	1100 <u>00000</u>
7	1000 <u>00000</u>

$\tau((S, D, R, C, M)) \notin \{0, \text{NaR}\}$ , characteristic  $c$  and regime  $r$ . Let  $\tilde{T} := (\tilde{S}, \tilde{D}, \tilde{R}, \tilde{C}, \tilde{M}) \in \{0, 1\}^n$  with characteristic  $\tilde{c}$ , regime  $\tilde{r}$  and arbitrary  $\tilde{S}$  and  $\tilde{M}$ . It holds  $\tilde{r} = r$  and  $\tilde{c} = -c - 1 = -c$  (in two's complement).

*Proof.* See Appendix A.  $\square$

As observed, negating the direction bit, the regime bits, and the characteristic bits corresponds to negating the characteristic value, which is represented in two's complement. This property can be leveraged in the following manner:

**Corollary 1** (conditional characteristic negation). *Let  $n \in \mathbb{N}_1$  and  $T := (S, D, R, C, M) \in \{0, 1\}^n$  as in Definition 1 with  $\tau((S, D, R, C, M)) \notin \{0, \text{NaR}\}$ , characteristic  $c$  and regime  $r$ . Let*

$$\tilde{T} := \begin{cases} (S, D, R, C, M) & D = 0 \\ (S, \tilde{D}, \tilde{R}, \tilde{C}, \tilde{M}) & D = 1 \end{cases} \quad (11)$$

with characteristic  $\tilde{c}$  and regime  $\tilde{r}$ . It holds  $\tilde{r} = r$  and

$$\tilde{c} = \begin{cases} c & D=0 \\ -c & D=1 \end{cases} = \begin{cases} -2^{r+1} + 1 + \sum_{i=0}^{r-1} C_i 2^i & D=0 \\ -2^{r+1} + 1 + \sum_{i=0}^{r-1} \tilde{C}_i 2^i & D=1. \end{cases} \quad (12)$$

*Proof.* This follows directly from Proposition 1 and Definition 1.  $\square$

This approach suggests a strategy for determining the characteristic  $c$ : First, conditionally negate the characteristic bits when the direction bit is 1. Next, apply the bias  $-2^{r+1}$  unconditionally, then increment the result. Finally, conditionally negate the intermediate result  $\tilde{c}$  when the direction bit is 1 to obtain the final characteristic  $c$ . This ensures that the process involves only incrementing in all cases (without any decrement), allowing us to focus solely on the single application of the bias  $-2^{r+1}$ .

Fortunately, the application of the bias is straightforward. As illustrated in Table I, each of the 8 possible biases can be added to the characteristic bits using a simple bitwise OR operation. Additionally, considering that the  $r$ th bit is always zero, it is theoretically possible to combine the incremented characteristic with the bias using this bitwise OR operation.

However, we adopt a different approach: Given that our raw characteristic contains the left-aligned characteristic

---

**Algorithm 1:** The process of determining the characteristic or the exponent from the raw characteristic (see Figure 3) and the antiregime depending on the direction bit.

---

**input :**  $characteristic\_raw\_bits \in \{0, 1\}^7$   
 $antiregime \in \{0, \dots, 7\}$   
 $direction\_bit \in \{0, 1\}$   
 $output\_exponent \in \{0, 1\}$

**output:**  $characteristic\_or\_exponent \in \{-255, \dots, 254\}$

**if**  $direction\_bit = 0$  **then**  
|  $characteristic\_raw\_normal\_bits \leftarrow$   
|  $characteristic\_raw\_bits$   
**else**  
|  $characteristic\_raw\_normal\_bits \leftarrow$   
|  $\neg characteristic\_raw\_bits$   
**end**  
 $characteristic\_precursor \leftarrow ((1, 0) \#$   
 $characteristic\_raw\_normal\_bits) \ggg antiregime$   
 $characteristic\_normal \leftarrow$   
 $(1) \# (characteristic\_precursor_{7,0} + 1)$   
**if**  $direction\_bit = output\_exponent$  **then**  
|  $characteristic\_or\_exponent \leftarrow$   
|  $characteristic\_normal$   
**else**  
|  $characteristic\_or\_exponent \leftarrow$   
|  $\neg characteristic\_normal$   
**end**

---

bits, we first invert these bits if the direction bit is 1. Next, we prepend the bits 10 to the left and perform an *arithmetic* right shift by the *antiregime* bits. This process yields the desired bitwise OR of the bias with the characteristic bits. Subsequently, we increment the first 8 bits of the resulting value, prepend 1 to the left, and then conditionally negate the outcome based on the direction bit, as illustrated in Corollary 1.

Referring back to the previously discussed internal representation in Section III, it was noted that in the case of linear takums, the exponent is obtained by negating the characteristic. Rather than performing this negation separately, which would introduce additional overhead, we introduce an additional input bit, *output\_exponent*. This bit, which is predetermined during synthesis and not a true input bit of the entity, inverts the conditional negation we already perform, thus providing the exponent negation at no extra cost.

The complete procedure is detailed in Algorithm 1. Note that, by convention, any vector with a negative length is considered an empty vector.

### B. Pre-, Logarithmic and Linear Decoder

We integrate these components into the predecoder, as outlined in Algorithm 2, to determine the sign, characteristic or exponent (depending on the value of *output\_exponent*), and mantissa. It is important to note

---

**Algorithm 2:** Predecoding of a given takum bit string of length  $n \in \mathbb{N}_2$  into sign, characteristic, mantissa bits and precision with additional detection of special cases 0 and NaR.

---

**input :**  $takum \in \{0, 1\}^n$   
 $output\_exponent \in \{0, 1\}$

**output:**  $sign\_bit \in \{0, 1\}$   
 $characteristic\_or\_exponent \in \{-255, \dots, 254\}$   
 $mantissa\_bits \in \{0, 1\}^{n-5}$   
 $precision \in \{0, \dots, n-5\}$   
 $is\_zero \in \{0, 1\}$   
 $is\_nar \in \{0, 1\}$

$sign\_bit \leftarrow takum_{n-1}$

$direction\_bit \leftarrow takum_{n-2}$

**if**  $n \geq 12$  **then**

|  $regime\_characteristic\_segment \leftarrow$   
|  $takum_{n-3, n-12}$

**else**

|  $regime\_characteristic\_segment \leftarrow$   
|  $takum_{n-3, 0} \# \mathbf{0}_{12-n} \in \{0, 1\}^{10}$

**end**

$regime\_bits \leftarrow$

$regime\_characteristic\_segment_{9,7}$

**if**  $direction\_bit = 0$  **then**

|  $regime \leftarrow \neg regime\_bits$   
|  $antiregime \leftarrow regime\_bits$

**else**

|  $regime \leftarrow regime\_bits$   
|  $antiregime \leftarrow \neg regime\_bits$

**end**

$characteristic\_raw\_bits \leftarrow$

$regime\_characteristic\_segment_{6,0}$

$characteristic\_or\_exponent \leftarrow$

$characteristic\_determinator(\$   
 $characteristic\_raw\_bits, antiregime,$   
 $direction\_bit, output\_exponent)$

$mantissa\_bits \leftarrow takum_{n-6, 0} \ll regime$

**if**  $regime < n - 5$  **then**

|  $precision \leftarrow (n - 5) - regime$

**else**

|  $precision \leftarrow 0$

**end**

$is\_zero \leftarrow takum = \mathbf{0}_n$

$is\_nar \leftarrow takum = (1) \# \mathbf{0}_{n-1}$

---

---

**Algorithm 3:** Decoding of a given (logarithmic) takum bit string of length  $n \in \mathbb{N}_2$  into sign, barred logarithmic value and precision with additional detection of special cases 0 and NaR.

---

**input :**  $takum \in \{0, 1\}^n$   
**output:**  $sign\_bit \in \{0, 1\}$   
 $barred\_logarithmic\_value \in \{0, 1\}^{n+4}$   
 $precision \in \{0, \dots, n - 5\}$   
 $is\_zero \in \{0, 1\}$   
 $is\_nar \in \{0, 1\}$

$sign\_bit, characteristic, mantissa\_bits, precision,$   
 $is\_zero, is\_nar \leftarrow \text{predecoder}(takum, 0)$

$barred\_logarithmic\_value \leftarrow$   
 $characteristic \# mantissa\_bits$

---



---

**Algorithm 4:** Decoding of a given linear takum bit string of length  $n \in \mathbb{N}_2$  into sign, exponent, fraction bits and precision with additional detection of special cases 0 and NaR.

---

**input :**  $takum \in \{0, 1\}^n$   
**output:**  $sign\_bit \in \{0, 1\}$   
 $exponent \in \{-255, \dots, 254\}$   
 $fraction\_bits \in \{0, 1\}^{n-5}$   
 $precision \in \{0, \dots, n - 5\}$   
 $is\_zero \in \{0, 1\}$   
 $is\_nar \in \{0, 1\}$

$sign\_bit, exponent, mantissa\_bits, precision,$   
 $is\_zero, is\_nar \leftarrow \text{predecoder}(takum, 1)$

$fraction\_bits \leftarrow mantissa\_bits$

---

that both  $n$  and  $output\_exponent$  are predetermined during synthesis, thereby eliminating many conditional operations.

For the decoding of logarithmic takums, as described in Algorithm 3, the predecoder output is utilised to concatenate the characteristic and mantissa, forming the barred logarithmic value. The linear decoder, detailed in Algorithm 4, leverages the predecoder to produce the internal representation described by (8). In this context, the input bit  $output\_exponent$  is set to 1 within the predecoder to directly yield the exponent instead of the characteristic.

## V. ENCODER

The objective of the encoder is to transform a given internal representation into the takum binary representation for a specified  $n \in \mathbb{N}_2$ . The internal representation is given by  $(S, e, f)$  in the linear case and by  $(S, \bar{\ell})$  in the logarithmic case, as defined in (8) and (10), respectively.

As discussed in Section III, both internal representations can be readily converted into the characteristic  $c$  and the mantissa  $m$  (where the fraction  $f$  corresponds to  $m$ ). Therefore, we can consider both representations as equivalent starting points for either case.

Table II: Ranges of characteristics characterising overflow and underflow for the special cases  $n \in \{2, \dots, 11\}$ . The rounding boundary (and the position of the rounding bit to the right of it) is indicated with a small gap.

$n$	last not underflowing	$c$	first overflowing	$c$
2	X0100000	-15	X11000000	15
3	X001000000	-63	X1110000000	63
4	X0001000000	-127	X11110000000	127
5	X00001000000	-191	X111110000000	191
6	X000001000000	-223	X1111110000000	223
7	X000000100000	-239	X11111110000000	239
8	X000000010000	-247	X111111110000000	247
9	X000000001000	-251	X11111111100000000	251
10	X000000000100	-253	X111111111100000000	253
11	X0000000000100	-254	X1111111111100000000	254

The direction bit  $D$  (denoted as  $direction\_bit$ ) can be straightforwardly determined by noting that it takes the value 1 when the characteristic satisfies  $characteristic \geq 0$ . Consequently, it can be assumed that the direction bit is readily available for further processing.

### A. Underflow/Overflow Predictor

Early in the process, it is crucial to predict whether the value we intend to encode might result in either an underflow or overflow, particularly since we are adhering to sticky arithmetic. Anticipating these potential outcomes early on enables us to significantly reduce the time on the critical path, as opposed to the alternative method of unconditionally rounding the sum at the end and subsequently checking for overflow or underflow.

To predict rounding, we can differentiate between two distinct cases. The first case occurs when  $n$  lies between 2 and 11. In this scenario, the rounding bit is positioned within the regime or characteristic, rendering the mantissa bits irrelevant. Instead, we establish bounds on the characteristic based on the value of  $n$ , as detailed in Table II. The sum that is closest to either 0 or NaR without causing an underflow represents an upper bound (excluding the boundary itself). Conversely, the first sum that overflows to 0 or NaR provides a lower bound (inclusive of the boundary itself).

The second scenario considers the case where  $n \geq 12$ . By construction, it is evident that a necessary condition for underflow and overflow occurs when the first 12 bits take the forms X000000000000 and X111111111111 respectively. This is because the direction bit and the regime bits being all zeros or all ones directly imply that the regime value is 7. Consequently, in the overflow scenario, the necessary condition  $c = -255$  or  $c = 254$  is satisfied.

To establish a sufficient condition for underflow or overflow, we must examine the mantissa bits. For underflow, these bits must be all zeros, and for overflow, they must be all ones, up to and including the rounding bit, which is consistently positioned since the regime value is always 7. Given that the bits preceding the mantissa have a fixed

---

**Algorithm 5:** Prediction if for the given characteristic and mantissa bits there is an overflow or underflow when rounding the final takum to  $n \in \mathbb{N}_2$  bits.

---

**input :**  $characteristic \in \{-255, \dots, 254\}$   
 $mantissa\_bits \in \{0, 1\}^{n-5}$

**output:**  $round\_down\_underflows \in \{0, 1\}$   
 $round\_up\_overflows \in \{0, 1\}$

**if**  $n \leq 11$  **then**  
   $characteristic\_bound \leftarrow$   
   $(15, 63, 127, 191, 223, 239, 247, 251, 253, 254)$   
   $round\_down\_underflows \leftarrow$   
   $(characteristic < -characteristic\_bound_{n-2})$   
   $round\_up\_overflows \leftarrow$   
   $(characteristic \geq characteristic\_bound_{n-2})$   
**else**  
  **if**  $mantissa_{n-6,6} = \mathbf{0}_{n-11}$  **then**  
  |  $round\_down\_underflows \leftarrow$   
  |  $(characteristic = -255)$   
  **else**  
  |  $round\_down\_underflows \leftarrow 0$   
  **end**  
  **if**  $mantissa_{n-6,6} = \mathbf{1}_{n-11}$  **then**  
  |  $round\_up\_overflows \leftarrow$   
  |  $(characteristic = 254)$   
  **else**  
  |  $round\_up\_overflows \leftarrow 0$   
  **end**  
**end**

---

length of 12, we need to inspect the  $n-11$  most significant mantissa bits.

In any instance where rounding down results in underflow, or rounding up leads to overflow, an output signal is generated to indicate the respective condition. The complete procedure is detailed in the pseudocode provided in Algorithm 5.

### B. Characteristic Precursor Determinator

The initial step in the encoding process involves determining the regime and characteristic bits from the given characteristic. To facilitate this, the characteristic is first normalised into a format that allows for the efficient extraction of both the regime and characteristic bits, regardless of the scenario. We refer to this specific format as the ‘characteristic precursor’. The characteristic precursor can be derived using the following

**Proposition 2** (characteristic precursor). *Let  $n \in \mathbb{N}_1$  and  $T := (S, D, R, C, M) \in \{0, 1\}^n$  as in Definition 1 with  $\tau((S, D, R, C, M)) \notin \{0, \text{NaR}\}$ , two’s complement characteristic  $c$  and regime  $r$ . It holds*

$$\begin{cases} -c & D = 0 \\ c & D = 1 \end{cases} + 1 = \begin{cases} 2^r + \sum_{i=0}^{r-1} \overline{C}_i 2^i & D = 0 \\ 2^r + \sum_{i=0}^{r-1} C_i 2^i & D = 1. \end{cases} \quad (13)$$

*Proof.* See Appendix B.  $\square$

---

**Algorithm 6:** Determination of the characteristic precursor using the direction bit and characteristic.

---

**input :**  $characteristic \in \{-255, \dots, 254\} \equiv \{0, 1\}^9$   
 $direction\_bit \in \{0, 1\}$

**output:**  $characteristic\_precursor \in \{0, 1\}^8$

**if**  $direction\_bit = 0$  **then**  
  |  $characteristic\_normal \leftarrow \neg characteristic_{7,0}$   
**else**  
  |  $characteristic\_normal \leftarrow characteristic_{7,0}$   
**end**  
 $characteristic\_precursor \leftarrow$   
 $characteristic\_normal + 1$

---

Refer to Algorithm 6 for the pseudocode implementation of the characteristic precursor determination. As can be observed, only the 8 least significant bits of the characteristic are negated. This approach stems from the fact that the normalised characteristic, by construction, always has a zero in the most significant bit. Consequently, the subsequent incrementation is performed on a ‘standard-form’ 8-bit bit string. It is important to note that employing the precursor enables us to circumvent a potentially necessary decrementation (see Definition 1), while the incrementation can be efficiently implemented using only half-adders.

However, it is crucial to bear in mind that the characteristic bits will need to be negated at a later stage. This step cannot be undertaken at the current moment, as the regime value  $r$  has not yet been extracted.

### C. 8-Bit Leading One Detector (LOD)

By construction, the characteristic precursor, represented as an 8-bit unsigned integer, possesses the highest integer power of  $2^r$  (refer to Proposition 2), where  $r$  denotes the regime. To determine the regime, it is necessary to employ an 8-bit leading one detector (LOD). We adopt the design proposed in [20], which divides the 8-bit number into two 4-bit segments. Each segment is then processed through a lookup table, which yields the offset value of the most significant bit set to 1.

If the most significant four bits are all zero, the result from the lower bits’ lookup table is returned. Conversely, if any of the highest four bits are set to 1, the result from the higher bits’ lookup table is returned, with 4 added to account for the fact that the leading one inherently has an offset of 4 due to its position. This adjustment ensures accurate determination of the regime. For a detailed implementation, refer to Algorithm 7.

### D. Takum with Rounding Bit Generator

The initial step in generating the takum with rounding bit, which has a length of  $n+1$ , involves deriving the regime bits from the regime. According to the definition, this process entails examining the direction bit. As detailed in Section V-B, the characteristic precursor must also be

---

**Algorithm 7:** A simple 8-bit leading one detector.

---

**input :**  $input \in \{0, 1\}^8 \setminus \mathbf{0}_8$   
**output:**  $leading\_one\_offset \in \{0, \dots, 7\}$   
 $lod4\_lut \leftarrow (0, 0, 1, 1, 2, 2, 2, 2, 3, 3, 3, 3, 3, 3, 3, 3)$   
**if**  $input_{7,4} = \mathbf{0}_4$  **then**  
  |  $leading\_one\_offset \leftarrow lod4\_lut_{input_{3,0}}$   
**else**  
  |  $leading\_one\_offset \leftarrow (1) \# lod4\_lut_{input_{7,4}}$   
**end**

---

**Algorithm 8:** Generation of an unrounded takum of length  $n + 1$  with  $n \in \mathbb{N}_2$  from the direction bit, regime, characteristic precursor and mantissa bits. The least significant bit is the rounding bit.

---

**input :**  $sign\_bit \in \{0, 1\}$   
 $direction\_bit \in \{0, 1\}$   
 $regime \in \{0, \dots, 7\}$   
 $characteristic\_precursor \in \{0, 1\}^8$   
 $mantissa\_bits \in \{0, 1\}^{n-5}$   
**output:**  $takum\_with\_rounding\_bit \in \{0, 1\}^{n+1}$   
**if**  $direction\_bit = 0$  **then**  
  |  $regime\_bits \leftarrow \neg regime$   
  |  $characteristic\_bits \leftarrow$   
  |  $\neg(characteristic\_precursor_{6,0})$   
**else**  
  |  $regime\_bits \leftarrow regime$   
  |  $characteristic\_bits \leftarrow$   
  |  $characteristic\_precursor_{6,0}$   
**end**  
 $characteristic\_mantissa\_bits \leftarrow$   
 $characteristic\_bits \# mantissa\_bits \# \mathbf{0}_7 \gg regime$   
 $takum\_with\_rounding\_bit \leftarrow$   
 $sign\_bit \# direction\_bit \# regime\_bits \#$   
 $characteristic\_mantissa\_bits_{n+1,6}$

---

inverted to obtain the coded characteristic bits, a task that coincidentally occurs during the direction bit check.

Upon inverting the characteristic precursor, the resulting characteristic bits are contained within the lower 7 bits of the output. Given that the characteristic bits vary in length from 0 to 7, there will be unused bits in the upper  $7 - regime$  bits. This is not problematic, as we subsequently combine these bits with the mantissa bits and 7 zero bits, then shift the entire sequence  $regime$  bits to the right. This ensures that the characteristic bits always start at index  $n + 1$  and are immediately followed by the mantissa bits, as intended.

Considering that the sign bit, direction bit, and three regime bits together occupy a total of 5 bits, we discard the lowest 6 bits of the shifted characteristic and mantissa bits. The remaining bits are then combined to form the desired output takum of length  $n + 1$ . The complete procedure is outlined in Algorithm 8.

It is noteworthy that the shifter, regardless of  $n$ , is con-

---

**Algorithm 9:** Rounding of the takum with rounding bit depending on the previously determined cases of rounding up and down yielding an under- or overflow.

---

**input :**  $takum\_with\_rounding\_bit \in \{0, 1\}^{n+1}$   
 $round\_up\_overflows \in \{0, 1\}$   
 $round\_down\_underflows \in \{0, 1\}$   
**output:**  $takum\_rounded \in \{0, 1\}^n$   
 $takum\_rounded\_up \leftarrow$   
 $takum\_with\_rounding\_bit_{n,1} + 1$   
 $takum\_rounded\_down \leftarrow$   
 $takum\_with\_rounding\_bit_{n,1}$   
**if**  $round\_up\_overflows = 0 \wedge$   
 $(takum\_with\_rounding\_bit_0 = 1 \vee$   
 $round\_down\_underflows = 1)$  **then**  
  |  $takum\_rounded \leftarrow takum\_rounded\_up$   
**else**  
  |  $takum\_rounded \leftarrow takum\_rounded\_down$   
**end**

---

strained by a maximum shift offset of 7 (i.e., three control bits) due to the limited tapering of the takum format. This contrasts sharply with posits, where the tapering is unbounded and a shifter must accommodate nearly the entire width  $n$ , which does not scale as effectively.

### E. Rounder

Having determined whether rounding up or down results in an overflow or underflow (see Section V-A), and having obtained the takum with the additional rounding bit (see Section V-D), we can now proceed to combine these elements to achieve a properly rounded takum.

The initial step involves generating two rounding candidates: one for rounding up and one for rounding down. The rounding-up candidate is obtained by incrementing the takum with the rounding bit, while the rounding-down candidate is derived by truncating the takum with the rounding bit to  $n$  bits, effectively removing the rounding bit.

We then perform a parallel check: we select the rounding-up candidate as the output if rounding up does not cause an overflow and if either the rounding bit is set or rounding down would result in an underflow. If these conditions are not met, we opt for the rounding-down candidate.

This approach is preferred over directly incrementing the takum with the rounding bit by the result of the logic expression, as it optimises timing: while we can immediately start incrementing and determining whether to round up or down as soon as the input arrives, direct incrementing would require waiting for the logic expression to evaluate before beginning the computation. A pseudocode implementation of this process is provided in Algorithm 9.

---

**Algorithm 10:** Postencoding process of a given sign, characteristic and mantissa bits into a takum of length  $n \in \mathbb{N}_2$  allowing the override for special cases 0 and NaR.

---

**input :**  $sign\_bit \in \{0, 1\}$   
 $characteristic \in \{-255, \dots, 254\}$   
 $mantissa\_bits \in \{0, 1\}^{n-5}$   
 $is\_zero \in \{0, 1\}$   
 $is\_nar \in \{0, 1\}$

**output:**  $takum \in \{0, 1\}^n$

$direction\_bit \leftarrow \neg characteristic_8$

$round\_down\_underflows, round\_up\_overflows \leftarrow$   
 $overflow\_underflow\_predictor($   
 $characteristic, mantissa\_bits)$

$characteristic\_precursor \leftarrow$   
 $characteristic\_precursor\_determinator($   
 $characteristic, direction\_bit)$

$regime \leftarrow$   
 $leading\_one\_detector\_8($   
 $characteristic\_precursor)$

$takum\_with\_rounding\_bit \leftarrow$   
 $takum\_with\_rounding\_bit\_generator($   
 $sign\_bit, direction\_bit, regime,$   
 $characteristic\_precursor, mantissa\_bits)$

$takum\_rounded \leftarrow$   
 $rounder($   
 $takum\_with\_rounding\_bit,$   
 $round\_up\_overflows, round\_down\_underflows)$

**if**  $is\_zero = 1 \vee is\_nar = 1$  **then**  
|  $takum \leftarrow (is\_nar) \# \mathbf{0}_{n-1}$   
**else**  
|  $takum \leftarrow takum\_rounded$   
**end**

---

#### F. Post-, Logarithmic and Linear Encoder

With all components in place, we can now integrate them into a single comprehensive algorithm: the postencoder. This algorithm accepts the sign, characteristic, and mantissa as inputs. The final step involves determining the direction bit at the outset, which is simply the inverted sign bit of the characteristic. Additionally, the algorithm must conditionally handle special cases when either of the input bits for 0 or NaR is set. The implementation of this process is detailed in pseudocode in Algorithm 10.

For encoding logarithmic takum values, as outlined in Algorithm 11, the characteristic and mantissa bits derived from the barred logarithmic value are passed into the postencoder. Similarly, the linear takum encoder, as described in Algorithm 12, employs the postencoder following the conversion of the internal representation from equation (8). The characteristic is computed from the exponent, with conditional negation applied based on  $S$ .

---

**Algorithm 11:** Encoding of given sign and barred logarithmic value into a (logarithmic) takum bit string of length  $n \in \mathbb{N}_2$ .

---

**input :**  $sign\_bit \in \{0, 1\}$   
 $barred\_logarithmic\_value \in \{0, 1\}^{n+4}$   
 $is\_zero \in \{0, 1\}$   
 $is\_nar \in \{0, 1\}$

**output:**  $takum \in \{0, 1\}^n$

$characteristic \leftarrow barred\_logarithmic\_value_{n+3, n-5}$   
 $mantissa\_bits \leftarrow barred\_logarithmic\_value_{n-6, 0}$

$takum \leftarrow postencoder(sign\_bit, characteristic,$   
 $mantissa\_bits, is\_zero, is\_nar)$

---



---

**Algorithm 12:** Encoding of given sign, exponent and fraction bits into a linear takum bit string of length  $n \in \mathbb{N}_2$ .

---

**input :**  $sign\_bit \in \{0, 1\}$   
 $exponent \in \{-255, \dots, 254\}$   
 $fraction\_bits \in \{0, 1\}^{n-5}$   
 $is\_zero \in \{0, 1\}$   
 $is\_nar \in \{0, 1\}$

**output:**  $takum \in \{0, 1\}^n$

**if**  $sign\_bit = 0$  **then**  
|  $characteristic \leftarrow exponent$   
**else**  
|  $characteristic \leftarrow \neg exponent$   
**end**

$takum \leftarrow postencoder(sign\_bit, characteristic,$   
 $fraction\_bits, is\_zero, is\_nar)$

---

## VI. EVALUATION

Having devised decoders and encoders for both logarithmic and linear takums, we now proceed to evaluate their performance relative to the most effective posit codecs. The synthesis was conducted using Vivado 2024.1 on a Kintex UltraScale+ KCU116 Evaluation Platform (part number xcku5p-ffvb676-2-e). We employed the default synthesis strategy (Vivado Synthesis Defaults, 2024) unless specified otherwise in the following evaluation.

Our codec is compared against the sign-magnitude FloPoCo codec (‘FloPoCo-SM’) [6]–[8], which utilizes the internal representation detailed in (7), and the enhanced two’s complement FloPoCo codec (‘FloPoCo-2C’) [9], which employs the optimised internal representation described in (8) and is integrated into the PERCIVAL RISC-V core project [10], [11]. For a comparison of the internal representations, refer to Section III.

The PACoGen codec [21] has been excluded from this comparison due to prior evidence indicating that its performance is generally inferior or at best comparable to that of the FloPoCo-2C codec, as demonstrated in [9, Figure 7]. Similarly, the MArTo codec [5] was not included for the same reason.

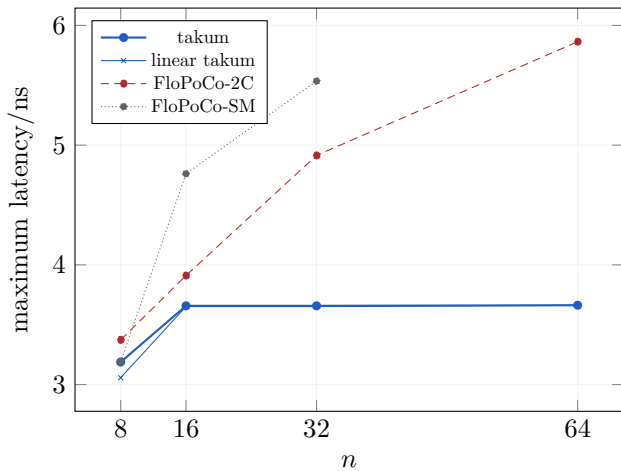


Figure 4: Maximum decoder latency.

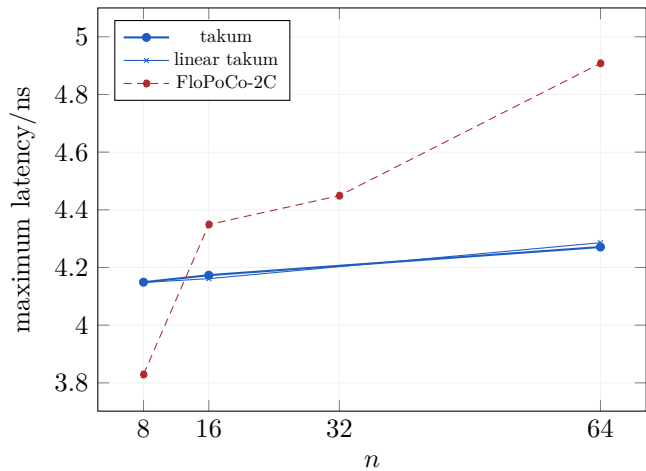


Figure 6: Maximum encoder latency.

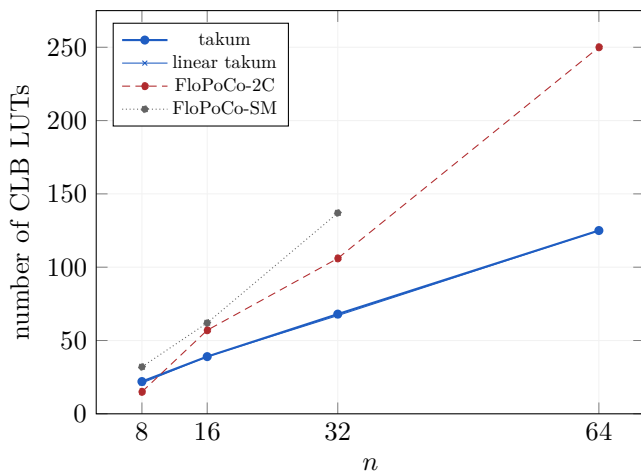


Figure 5: Decoder CLB LUT consumption.

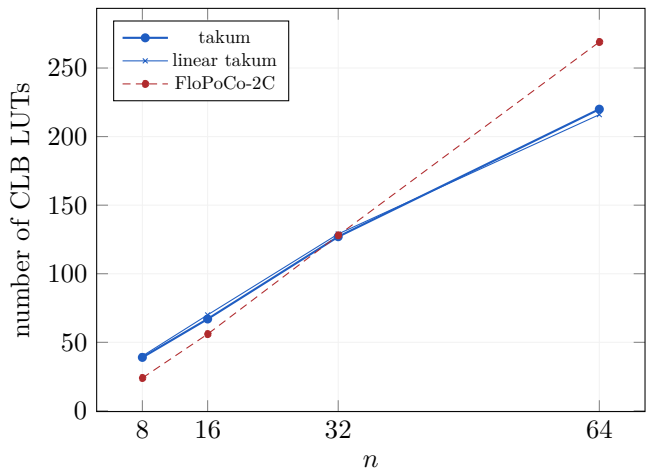


Figure 7: Encoder CLB LUT consumption.

### A. Decoder

We begin by assessing the decoder’s performance by measuring its maximum latency and CLB LUT consumption on the reference FPGA. With respect to maximum latency, as illustrated in Figure 4, it is noteworthy that our results for both FloPoCo-SM and FloPoCo-2C are consistent with those reported in [9].

The results indicate that the takum decoders consistently outperform both reference decoders, demonstrating a constant delay irrespective of increasing  $n$ . Although FloPoCo-2C surpasses FloPoCo-SM across all tested values of  $n$ , FloPoCo-SM exhibits a lower latency for  $n = 8$ . Nonetheless, the takum decoders achieve a latency lower or comparable to that of the FloPoCo-SM decoder in this instance.

A similar trend is observed in the CLB LUT consumption, as shown in Figure 5. For  $n = 8$ , all three implementations exhibit comparable CLB LUT usage and nearly linear delay growth. However, the takum decoder demonstrates a significantly lower CLB LUT consumption, with only half the usage compared to the most efficient

posit reference.

### B. Encoder

In our comparison of encoders it is important to note that FloPoCo-SM is not included. This omission is due to the fact that FloPoCo-SM lacks a distinct posit encoder within its codebase that could be evaluated separately. Instead, the posit encoder is integrated with the arithmetic logic in FloPoCo-SM. Additionally, while the takum encoders incorporate comprehensive rounding logic, the FloPoCo-2C encoder depends on external rounding information provided by the caller, which must be determined independently beforehand. Consequently, the intrinsic overhead associated with the takum encoder is also present in the FloPoCo-2C encoder; however, this overhead is part of the arithmetic logic and, therefore, not measured in this study.

Moreover, for  $n = 16$ , the synthesiser defaults to using Look-Up Tables (LUTs) instead of a CARRY8 chain for computing *takum\_rounded\_up* (refer to Algorithm 8). This choice increases the delay and may be considered

a software bug. To address this, synthesis settings were adjusted to enforce the use of a CARRY8 chain.

Examining the maximum latency shown in Figure 6, it is observed that while the takum encoders exhibit higher latency for  $n = 8$ , their latencies increase only slightly with larger  $n$ . In contrast, the latency of the FloPoCo-2C encoder increases more significantly as  $n$  grows. The logarithmic and linear variants of the takum encoder demonstrate similar performance characteristics across different values of  $n$ .

In terms of slice LUT consumption, as illustrated in Figure 7, the takum and posit encoders show comparable usage. The posit encoder exhibits a slight advantage for smaller values of  $n$ , whereas the takum encoder has a marginal advantage for larger  $n$ .

## VII. CONCLUSION AND OUTLOOK

We have demonstrated the design and implementation of a takum hardware codec using VHDL, proposing a new internal LNS representation for improved performance. Our evaluations reveal that the takum codec either outperforms or matches the performance of the leading posit codec, FloPoCo-2C. This superior performance can largely be attributed to the fact that the exponent encoding length in takums is bounded, whereas for posits, it is unbounded. Consequently, posits require logic that encompasses the entire width of the binary string—spanning all bits during both decoding and encoding operations (e.g., shifts), rather than just the initial 12 bits. Therefore, takums are generally more hardware-efficient compared to posits on FPGA platforms.

Future work will involve evaluating the performance of the takum codec on VLSI systems, given that the complexity of FPGA implementations does not always correlate directly with VLSI complexity. Furthermore, it is warranted to investigate the effects of the novel choice of base  $e$  in (logarithmic) takums on the hardware implementation of an arithmetic core. This aspect is tentatively addressed in [15, Section 4.4], which builds upon the foundational work presented in [22]. However, a comprehensive hardware implementation is necessary for a thorough assessment.

## REFERENCES

- [1] S. Wang and P. Kanwar, ‘Bfloat16: The secret to high performance on cloud tpus,’ Aug. 2019. [Online]. Available: <https://web.archive.org/web/20190826170119/https://cloud.google.com/blog/products/ai-machine-learning/bfloat16-the-secret-to-high-performance-on-cloud-tpus>
- [2] J. L. Gustafson and I. Yonemoto, ‘Beating floating point at its own game: Posit arithmetic,’ *Supercomputing Frontiers and Innovations*, vol. 4, no. 2, pp. 71–86, Jun. 2017. DOI: 10.14529/jsfi170206.
- [3] J. L. Gustafson, G. Bohlender, S. Y. Chung *et al.*, ‘Standard for Posit™ arithmetic,’ Mar. 2022. [Online]. Available: [https://web.archive.org/web/20220603115338/https://posithub.org/docs/posit\\_standard-2.pdf](https://web.archive.org/web/20220603115338/https://posithub.org/docs/posit_standard-2.pdf)
- [4] R. Chaurasiya, J. Gustafson, R. Shrestha *et al.*, ‘Parameterized posit arithmetic hardware generator,’ in *2018 IEEE 36th International Conference on Computer Design (ICCD)*, 2018, pp. 334–341. DOI: 10.1109/ICCD.2018.00057.
- [5] Y. Uguen, L. Forget and F. de Dinechin, ‘Evaluating the hardware cost of the posit number system,’ in *2019 29th International Conference on Field Programmable Logic and Applications (FPL)*, 2019, pp. 106–113. DOI: 10.1109/FPL.2019.00026.
- [6] R. Murillo, A. A. Del Barrio and G. Botella, ‘Customized posit adders and multipliers using the FloPoCo core generator,’ in *2020 IEEE International Symposium on Circuits and Systems (ISCAS)*, IEEE, 2020, pp. 1–5. DOI: 10.1109/ISCAS45731.2020.9180771.
- [7] R. Murillo, A. A. Del Barrio, G. Botella, M. S. Kim, H. Kim and N. Bagherzadeh, ‘PLAM: A posit logarithm-approximate multiplier,’ *IEEE Transactions on Emerging Topics in Computing*, pp. 2079–2085, 2021. DOI: 10.1109/TETC.2021.3109127.
- [8] R. Murillo, D. Mallasén, A. A. Del Barrio and G. Botella, ‘Energy-efficient MAC units for fused posit arithmetic,’ in *2021 IEEE 39th International Conference on Computer Design (ICCD)*, IEEE, 2021, pp. 138–145. DOI: 10.1109/ICCD53106.2021.00032.
- [9] R. Murillo, D. Mallasén, A. A. Del Barrio and G. Botella, ‘Comparing different decodings for posit arithmetic,’ in *Conference on Next Generation Arithmetic*, Springer, 2022, pp. 84–99. DOI: 10.1007/978-3-031-09779-9\_6.
- [10] D. Mallasén, R. Murillo, A. A. D. Barrio, G. Botella, L. Piñuel and M. Prieto-Matias, ‘PERCIVAL: Open-source posit RISC-V core with quire capability,’ *IEEE Transactions on Emerging Topics in Computing*, vol. 10, no. 3, pp. 1241–1252, 2022. DOI: 10.1109/TETC.2022.3187199.
- [11] D. Mallasén, A. A. Del Barrio and M. Prieto-Matias, ‘Big-PERCIVAL: Exploring the native use of 64-bit posit arithmetic in scientific computing,’ *IEEE Transactions on Computers*, vol. 73, no. 6, pp. 1472–1485, Jun. 2024. DOI: 10.1109/TC.2024.3377890.
- [12] Z. Carmichael, H. F. Langroudi, C. Khazanov, J. Lillie, J. L. Gustafson and D. Kudithipudi, ‘Deep positron: A deep neural network using the posit number system,’ in *2019 Design, Automation & Test in Europe Conference & Exhibition (DATE)*, 2019, pp. 1421–1426. DOI: 10.23919/DATE.2019.8719202.
- [13] A. Ramachandran, Z. Wan, G. Jeong, J. L. Gustafson and T. Krishna, ‘Algorithm-hardware co-design of distribution-aware logarithmic-posit encodings for efficient DNN inference,’ pp. 1–6, Mar. 2024. arXiv: 2403.05465 [cs.HA].
- [14] F. de Dinechin, L. Forget, J.-M. Muller and Y. Uguen, ‘Posits: The good, the bad and the ugly,’ ser. CoNGA-19, Singapore, Singapore: Association for Computing Machinery, 2019. DOI: 10.1145/3316279.3316285.

- [15] L. Hunhold, ‘Beating posits at their own game: Takum arithmetic,’ pp. 1–72, Apr. 2024, In publication. arXiv: 2404.18603 [math.NA].
- [16] J. N. Coleman, E. I. Chester, C. I. Softley and J. Kadlec, ‘Arithmetic on the european logarithmic microprocessor,’ *IEEE Transactions on Computers*, vol. 49, no. 7, pp. 702–715, 2000. DOI: 10.1109/12.863040.
- [17] D. Miyashita, E. H. Lee and B. Murmann, ‘Convolutional neural networks using logarithmic data representation,’ pp. 1–10, Mar. 2016. arXiv: 1603.01025 [cs.NE].
- [18] J. N. Coleman and R. Che Ismail, ‘Lns with co-transformation competes with floating-point,’ *IEEE Transactions on Computers*, vol. 65, no. 1, pp. 136–146, 2016. DOI: 10.1109/TC.2015.2409059.
- [19] M. S. S. M. Basir, R. Che Ismail and S. Z. M. Naziri, ‘An investigation of extended co-transformation using second-degree interpolation for logarithmic number system,’ pp. 59–63, 2020. DOI: 10.1109/FORTEI-ICEE50915.2020.9249931.
- [20] Z. Ebrahimi, D. Klar, M. A. Ekhtiyar and A. Kumar, ‘Plasticine: A cross-layer approximation methodology for multi-kernel applications through minimally biased, high-throughput, and energy-efficient SIMD soft multiplier-divider,’ *ACM Transactions on Design Automation of Electronic Systems (TODAES)*, vol. 27, no. 2, Nov. 2021. DOI: 10.1145/3486616.
- [21] M. K. Jaiswal and H. K.-H. So, ‘PACoGen: A hardware posit arithmetic core generator,’ *IEEE Access*, vol. 7, pp. 74586–74601, 2019. DOI: 10.1109/ACCESS.2019.2920936.
- [22] J.-M. Muller, ‘Discrete basis and computation of elementary functions,’ *IEEE Transactions on Computers*, vol. 34, no. 09, pp. 857–862, Sep. 1985. DOI: 10.1109/TC.1985.1676643.

#### APPENDIX A

##### PROOF OF PROPOSITION 1

It follows by definition that  $\tilde{r} = r$  given the negation of the direction bit corresponds with the negation of the regime bits, yielding the same regime value. For the characteristic values we consider the following two cases:

Case 1 ( $\overline{D} = 0$ ):

$$\tilde{c} = -2^{r+1} + 1 + \sum_{i=0}^{r-1} \overline{C}_i 2^i \quad (14)$$

$$= -2^{r+1} + 1 + \left( (2^r - 1) - \sum_{i=0}^{r-1} C_i 2^i \right) \quad (15)$$

$$= -2^r + 1 - \left( \sum_{i=0}^{r-1} C_i 2^i \right) - 1 \quad (16)$$

$$= - \left( 2^r - 1 + \sum_{i=0}^{r-1} C_i 2^i \right) - 1 \quad (17)$$

$$= -c - 1 \quad (18)$$

Case 2 ( $\overline{D} = 1$ ):

$$\tilde{c} = 2^r - 1 + \sum_{i=0}^{r-1} \overline{C}_i 2^i \quad (19)$$

$$= 2^r - 1 + \left( (2^r - 1) - \sum_{i=0}^{r-1} C_i 2^i \right) \quad (20)$$

$$= 2^{r+1} - 1 - \left( \sum_{i=0}^{r-1} C_i 2^i \right) - 1 \quad (21)$$

$$= - \left( -2^{r+1} + 1 + \sum_{i=0}^{r-1} C_i 2^i \right) - 1 \quad (22)$$

$$= -c - 1 \quad (23)$$

As both cases yield  $\tilde{c} = -c - 1$  and  $\neg c = -c - 1$  holds for two’s complement negation we have proven what was to be shown.  $\square$

#### APPENDIX B

##### PROOF OF PROPOSITION 2

We consider the following two cases:

Case 1 ( $D = 0$ ):

It holds for any two’s complement signed integer  $k \in \mathbb{Z}$  that  $\neg k + 1 = -k$ . Likewise we know that  $\neg k = -k - 1$  holds (a). We also know that for any unsigned  $m$ -bit integer  $\ell \in \mathbb{N}_0$  it holds  $\neg \ell = 2^m - 1 - \ell$  (b). It follows:

$$\neg c + 1 \stackrel{a}{=} (-c - 1) + 1 \quad (24)$$

$$= -c \quad (25)$$

$$= - \left( -2^{r+1} + 1 + \sum_{i=0}^{r-1} C_i 2^i \right) \quad (26)$$

$$= 2^{r+1} - 1 - \sum_{i=0}^{r-1} C_i 2^i \quad (27)$$

$$\stackrel{b}{=} 2^{r+1} - 1 - \left( 2^r - 1 - \sum_{i=0}^{r-1} \overline{C}_i 2^i \right) \quad (28)$$

$$= 2^r + \sum_{i=0}^{r-1} \overline{C}_i 2^i. \quad (29)$$

Case 2 ( $D = 1$ ):

$$c + 1 = 2^r - 1 + \left( \sum_{i=0}^{r-1} C_i 2^i \right) + 1 \quad (30)$$

$$= 2^r + \sum_{i=0}^{r-1} C_i 2^i \quad (31)$$

As both cases yield the desired results we have proven what was to be shown.  $\square$